Journal of Harbin Engineering University Vol 45 No. 4
ISSN: 1006-7043 April 2024

Polyethylene Terephthalate-Reduced Graphene Oxide Composites: Synthesis and Characterization

Gyanesh Katiyar[1*], Kavita Srivastava[2] , Dr. Deepak Srivastava[1]
[1]*Department of Plastic Technology, School of Chemical Technology, H B Technical University, Kanpur – 208 002 (U.P.), India.*
[2]*Department of Chemistry, V S S D College, Kanpur – 208 002 (U.P.), India.*

Abstract. A promising method for large-scale production is the polymerization process in the presence of GO dispersion combined with in situ GO reduction. By using in situ melt poly-condensation of poly ethylene terephathalate and simultaneous reduction of injected graphene oxide, a composite of poly ethylene terephathalate packed with reduced graphene oxide was produced. Rotational rheometry was used to perform the rheological test, which was then contrasted with virgin poly ethylene terephthalate. Differential scanning calorimetry was used to study the melting and crystallization of the reduced graphene oxide-polyethylene terephthalate composite. The morphology of the reduced graphene oxide–polyethylene terephthalate composite was investigated using optical microscopy. The reduced graphene oxide was separated from the reduced graphene oxide–polyethylene terephthalate composite using thermo gravimetry, X-ray photoelectron spectroscopy, and X-ray diffraction techniques. Polyethylene terephthalate is predicted to graft onto the reduced graphene oxide sheets because tri-fluoro acetic acid was unable to extract all of the polymer from the reduced graphene oxide particles. The rheological behavior of the melted reduced graphene oxide-poly ethylene terephthalate composite supports this theory.
Key Words: Thermo gravimetry, X-ray diffraction, polyethylene terephathalate, rheometry and reduced graphene oxide

Introduction

As a filler for polymer composites, graphene, fabricated from sp^2 carbon honeycombs and possessing exceptional mechanical and electrical properties, received significant attention in the last year. Due to strong stacking interactions [1], graphene tends to aggregate. Due to its poor dispersibility, graphene is not easily spread. To achieve exceptional properties in polymer graphene composites, the size of particles and the qualitative distribution of graphene plates within a polymeric matrix are crucial, making this task arduous. The most prevalent way to create graphene is through the reduction of exfoliated graphene oxide (GO). In general, the Hummers approach [2] yields GO, which is transformed from graphite using powerful oxidizing agents like KMO_4, H_2SO_4, and $NaNO_3$. The oxidation process involves the attachment of many functional oxygen groups to the basal planes and edges of graphene sheets. The gap between graphene sheets in GO expands as the distance between them increases, unlike graphite. GO is hydrophilic and can be easily dispersed in water and polar organic solvents on single layers or even multiple layers through simple sonication [3]. RGO, which is a type of reduced GO compound, can be produced through reduction. RGO was typically produced through chemical, thermal, solvo-thermal, and electrochemical reduction methods. The reduction of GO in chemical terms is often achieved through the use of hydrozine, ascorbic acid, or sodium borohydride. Solicitation of GO dispersion in appropriate solvent at high temperatures is known as the solubility of gas [4].

The loss of oxygen containing functional groups that facilitate the interaction between graphene nanosheets and solvent or polymer matrix causes nonfunctionalized RGO to have poor dispersibility in a polymeric matrix. Several in situ reduction methods were utilized to resolve this limitation. RGO polymer composites are commonly produced through the chemical reduction of GO in a polymeric solution or dispersion [1,5]. The reduction of GO in polymer composites was described as occurring after chemical [3] or thermal treatment [6-7]. The combination of in situ GO reduction and polymerization through presence

DISpersion offers great promise for large-scale production. Polycondensation was a successful method for preparing composites such as polyimide [8,9], polyamide [10] and polyethylene terephthalate (PET) [11]. These two techniques are now widely used. The use of melt processing for composites is more economically and environmentally advantageous than solution-based processes, as there is no need to recover solvents.
In situ poly condensation with simultaneous reduction of GO is used to prepare RGO PET composites. This study investigates these materials. How do they work. After being separated from the polymer matrix, RGO was subjected to thermo gravimetry (TGA), XPS, and XRD analysis. They also tested thermal properties of the RGO PET composite and rheological properties for the melts produced from RGO PET, respectively.

Experimental part:

Materials:

Sulfuric acid, hydrochloric acid, tri-fluoroacetic acid, sodium permanganate, dimethylformamide (DMF), potassium hydroxide, sodium, hydrogen peroxide, stibium oxide (III) and ethanol of reagent grade purity were used without additional purification. All solvents, acids and alkalis were purchased. Thionyl chloride (reagent grade) was distilled before application. Toluene was refluxed for 3 h over sodium and distilled. Pyridine was refluxed for 6 h with KOH and distilled. The purified graphite for GO preparation was ground by a mill and sifted through standard 0.08 mm mesh sieves. Deionized water (DI) with specific electro conductivity less than 1μSm/cm was used. Dichloracetic acid (DCA) for intrinsic and specific viscosity measurements has analytical grade purity. Terephthalic acid (TA), ethylene glycol (EG) and industrial polyethylene terephthalate containing 0.2 % isophthalic acid were obtained. Ethylene glycol was used for synthesis of bis-(2-hydroxyethyl) terephthalate and distilled over sodium.

Synthesis and exfoliation of GO:

Oxidation of graphite was carried out according to modified Hummer's method, using a mixture of $KMnO_4/H_2SO_4/H_3PO_4$ [12]. GO aqueous dispersion was prepared by mixing of 0.199 g GO in 25 ml DI water with IKA T10 Basic Ultra-Turrax disperser for 30 min. The viscous dark-brown dispersion was filtered through 0.45 μm PTFE filter.

Terephthaloyl dichloride chemical reaction:

TA (0.352 mol), $SOCl_2$ (1.52 mol) were refluxed in presence of few drops of DMF during 8 h. Excess of $SOCl_2$ was distilled out, and a residue was recrystallized from anhydrous toluene (m.p. 82-83°C).

Synthesis of bis(2-hydroxyethyl) terephthalate (BHET):

A flask with a magnetic stirrer, containing EG (110 g) was cooled by ice bath for 30 min, and 0.235 mole of terephthaloyl dichloride was charged into the flask. Anhydrous pyridine (0.47 mole) was then added dropwise to the reaction mixture for 10 min. The ice bath was removed, the reaction mixture was heated and kept for 2 h at 40°C. White precipitate was filtered on Büchner funnel, repeatedly washed with water and dried.

Poly dispensing of RGO PET:

BHET (39.5 g), Sb_2O_3 catalyst (10 mg) were charged into a 250 ml three-neck round bottom flask equipped with a mechanical glass paddle stirrer, an argon inlet and a vacuum outlet. Aqueous GO dispersion (25 ml) containing 0.199 g of GO was mixed with EG (25 ml) and poured into the flask. The flask was immersed into the wood bath preheated to 130-150° C and kept there for about 30-40 min until most of the water was distilled out. In order to remove the excess of EG, the wood bath was heated to 230°C for about 40 min in slow flow argon. Then, the temperature of the wood bath was raised to 270-280°C and the vacuum was applied (~1 Torr). After about 11 h of poly-condensation, the RGO- PET was evacuated from the flask under the stream of argon and cooled on air. The intrinsic viscosity of the RGO-PET was 1.0 dl/g in DCA at 25°C.

Separation of RGO and RGO-PET:

The RGO-PET (1.00 g) was dissolved in about 20 ml of TFA, filtered through a 0.22 μm polypropylene membrane filter and dried. The filtrate was thoroughly washed with fresh TFA and air dried. The yield was 25 mg (2.5%).

Thermal absorption of GO (RGO 300):

The sample of GO (100 mg) was placed in a round bottom flask. The flask was immersed into the wood bath and kept for 1 h at 300°C under slow flow of argon.

The characterization process:

Intrinsic and specific viscosity were measured in DCA at 25°C using Ubbelode viscometer.X-ray diffraction patterns were obtained with Rigaku Rotaflex RU-200 X-ray source with a rotating copper anode (Cu Kα–radiation with characteristic wavelength λ=1.542 Å, a secondary curved graphite monochromator was used) at apparatus operating conditions 50 kV–160 mA. The unit was equipped with a horizontal wide-angle goniometer Rigaku D/MAX-RC using Bragg-Brentano scheme in θ-2θ geometry. Scanning was carried out in the 3-40 angle range at 2θ scale with a speed of 1°/min and 0.04° increment. A scintillation counter was used as a detector of diffracted X-ray emission. XRD studies were carried out at room temperature.

XPS of the samples surface was carried out with the electron-ion spectroscopy module based on Nanofab 25 (NT-MDT) platform in ultrahigh oil-free vacuum (10–6 Pa). The X-ray source SPECS XR 50 without a monochromator with Mg anode as the X-ray source (1253.6 eV photon energy) was used. The spectra were registered with an electrostatic hemispherical energy analyzer SPECS Phoibos 225. The energy resolution based on the full width at half maximum (FWHM) of the spectrometer at the Ag3d5/2 line (peak) was 0.78 eV for non-monochromatic X-radiation Mg Kα. The energy positions of the spectra were calibrated with reference to the Cu2p3/2 (binding energy 932.62 eV), Ag3d5/2 (368.21 eV) and Au4f7/2 (83.95 eV) peaks. All survey spectra scans were recorded at the pass energy of 80 eV. The TGA measurements were carried out using TGA / DSC combined thermal analysis instrument, Mettler Toledo (Switzerland), in 70 µl alumina crucible at the heating rate of 10 °C / min from 30 to 1000 °C under 10 cm3/min flow rate of argon.

The differential scanning calorimetry (DCS) measurement was performed by DSC 823e Mettler Toledo (Switzerland) in 40 µl aluminum crucibles without perforation at the heating/cooling rate of 10 °C/min (30-300°C) under 70 ml/min flow rate of argon. The crystallization was studied at first cooling from 300°C to 30°C. The melting point and enthalpy were determined at second heating.

The degree of crystallinity X_c of PET and RGO-PET was measured using the following equation:

$X_c = \Delta H_f$ (PET) / ΔH_f0 (PET) ×{W(PET)}-1.100% (1)

where ΔH_f0 (PET) =$140Jg^{-1}$ and W(PET) is the weight fraction of pet [13] he graphene concentration Xg (TGA) in RGO was calculated from TGA using the following equation:

X_g (TGA) = RRGO - RPET / RGO - RPET × 100% (2)

where RRGO, RPET and RGO are ratio of weight at 500 °C to weight at 300 °C for RGO, GO, and PET respectively.

The graphene concentration Xg (XPS) in RGO was calculated from XPS measurements using the following equation:

$$X_g(XPS) = \frac{\omega(C)_g - \omega(C)_{RGO}}{\omega(C)_g - \omega(C)_{PET}} \times 100\% \quad (3)$$

where ω(c)RGO, ω(c)G = 78%, ω(c)PET = 65% are weight fraction of carbon in RGO, graphene and PET respectively.

The rheological properties of melts at steady state shear flow were studied on a RS600 rotational rheometer (Thermo Haake, Germany) using a plate–plate operation unit at 270 °C in the shear rate range of 101-103 $s^{-1.}$

Morphological study of the RGO-PET thin film (about 10 µm) was performed using a Biomed 6 PO polarization optical microscope. The thin film was prepared by drying of the RGO-PET solution in TFA on air.

Results And Discussion:

Stable dispersion of GO is observed in different types of highly charged compounds, as previously mentioned. Even so, the exceptional dispersibility of GO in water-mistaken solvents has led to the use of solvent exchange as a means of preparation. In a poly condensation flask, we employed the solvent exchange method in situ as well. Exfoliated GO, water, excess of EG, and BHET were used to start poly condensation. What was the starting material?

GO had a weight of 0. 5% w/w when measured against the monomer (BHET). Synthesis of RGO PET consists of several stages. Initially, the water was extracted from the poly condensation flask by distilling. A slow release of argon at elevated temperatures was used to eliminate the excess energy from EG. EG has a much higher boiling point (197°C) than water and the water was easily evaporated at 100°C by distillation, and in the second step the GO reducing caused the reaction media to turn black. After removing the majority of EG, the mixture was heated to 280°C under reduced pressure and constant stirring to remove volatile by product of poly condensation. Poly condensation was halted when the media became too viscous to stir.

To examine the RGO found in the composite RNO, a 0. 22 m membrane filter was used to dissolve the weighted Rgo PET sample in TFA. TGA, XRD, and xPS were employed to analyze the isolated RGO (2. 5% w/w). The study included multiple samples. Additionally, the chemical composition of RGO 300, a thermally reduced GO at 300°C, was studied through XPS.Figure 1 and Table 2 contain the TGA data for GO, PET, RGO PET products, and Rgo. GO exhibits thermal instability and can lose weight even at temperatures below 100°C (3%). At 160 225°C (43%), the most significant weigh loss of all observed data was GO. These are not the same as those provided in [14,15]. The weight loss results in 10% at 100°C and 20% when 200 (Zhou et al.) above the temperature threshold, which is dependent on the graphite oxidation method used and post-treatment processes such as drying. While GO and RGO PET showed that they could not lose their mass below 300°C, respectively, the former was 49. 5% and the latter was 11. 4% with respect to temperature. This is observed as the GO (weight) loss due to the elimination of certain functional groups of oxygen, and also because RGO weight lost due "to removal of TFA", which was used for isolation of RGO[I]. Despite being performed in ultrahigh vacuum, TFA was not detected in RGO using the XPS method (10 Pa). Consequently, it was determined that TFA was initially bound to RGO through Van der Waals or hydrogen bonds and then extracted in vacuum. RGO, neat PET and RGO-PET experienced a significant mass loss at temperatures ranging from 400 500°C. The peculiar thermal behavior of RGO indicates the existence of PET even after thorough purification. '" Therefore, the RGO sheets were made functional by PET during the polycondensation process. The assumption that RGO is made of PET and graphene combined result in the calculation of the weight fraction of grafted polymer in RGB. Assuming a poly condensation process at 280°C, the second assumption is that graphene in RGO exhibits thermal behavior equivalent to GO at temperatures above 300 C.

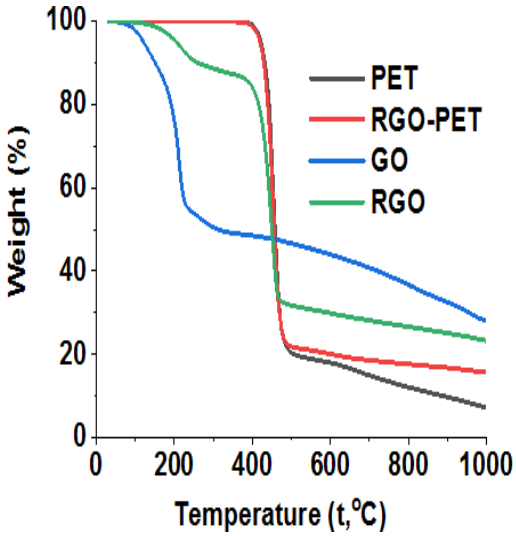

Figure 1. TGA curves of GO, RGO, neat PET, RGO-PET

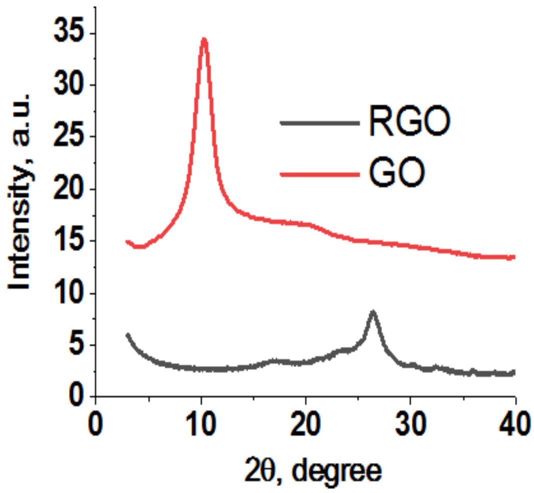

Figure 2. XRD pattern of GO and RGO

Table 1. Mass loss of GO, RGO, RGO-PET and PET after heating from 300 °C to 500 °C and from 300 °C to 1000°C.

Temperature range	Residual weight, %			
	GO	RGO	RGO-PET	PET
300-500	92.8	35.8	21.9	20.4
300-1000	55.6	26.3	15.6	7.2

The XRD pattern of RGO and GO is shown in figure 2. The main reflex of GO appears at 10.3° corresponding to the interplanar distance between the graphene sheets equal to 0.858 nm. The diffraction peak of RGO is located at 26.4°. The presence of PET in RGO was revealed as a wide diffraction peak at about 20°, which was previously reported in [16].

The elemental analysis of GO, RGO, and RGO-300 was performed by the XPS method as it was described in [17]. The results are presented in Table 2.

Table 2. Relative atomic concentration of C and O in GO, RGO-300, and RGO

Elements	GO, %	RGO, %	RGO-300	
C	67.9	76.4	82.2	
O	27.4	23.6	17.8	
S	2.2	–	–	
N	2.5	–	–	

According to the PET formula, C/O ratio in PET is 2.5. Thermally reduced GO (RGO-300) contains 82.2% of carbon. Assuming that RGO sheets should consist of 82.2% carbon, the calculated by equation (3) weight fraction of PET in RGO is 55%, which is lower compared to the results based on TGA (80%). The reduction of GO in poly condensation melt is different from thermal reduction of GO due to the presence of a reducing reagent such as EG and acetaldehyde. We suppose RGO is more reduced than RGO-300 and that the XPS method underestimates PET content in RGO. As mentioned above, the weight concentration of RGO in RGO-PET is 2.5%. Relying on the TGA results, the true concentration of graphene in RGO-PET is about 0.5%.

Grafting of RGO with PET also was proved by swelling in two different solvents. There was swelling of RGO in TFA which is a solvent of PET and no swelling in $CHCl_3$ (figure 3).

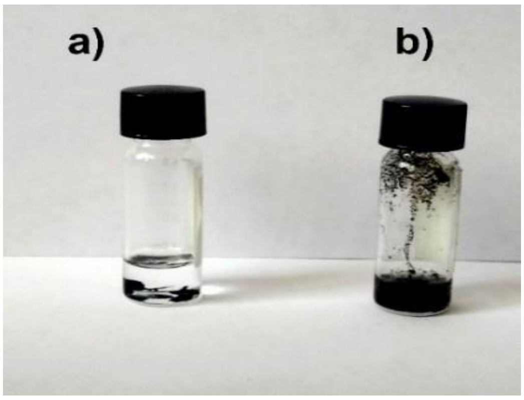

Figure 3. Swelling of RGO in CHCl3 (a) and in TFA

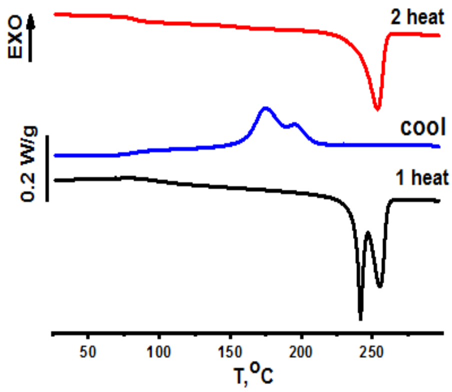

(b)DSC thermograms are presented in figure 4 and summarized in Table 3. The degree of crystallinity Xc and crystallization temperature Tc of RGO-PET are higher than Xc and Tc of neat PET. The increasing of Xc and Tc was also observed for PET/RGO composites prepared by mixing PET and RGO [16,18]. Glass transition temperature T_g and melting temperature Tm of RGO-PET are lower than that of PET.

(a)

(b)

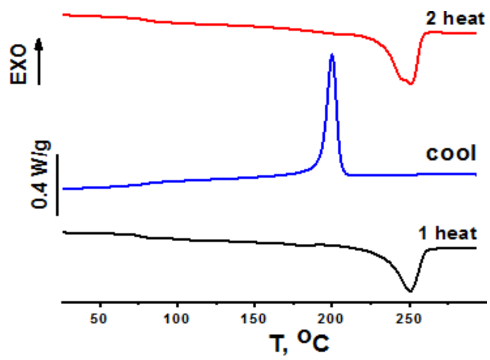

Figure 4. DSC thermogram of pristine PET (a) and

RGO-PET (b)

Table 3. DSC results for RGO-PET and PET

Sample	T_g, °C	T_c, °C	T_m, °C	ΔH_f, J/g	X_c, %
PET	81.2	174.9	253.5	41.15	29.5
RGO-PET	77.4	205.6	250.8	42.78	30.7

The morphological characteristics of the polymer composite were observed through optical microscopy (figure 5). The obtained images enable us to observe a fairly even distribution of particles across the polymer volume. The maximum size of an agglomerate is 50 m.A polymer that creates fibers has been the customary substance in PET. Measured to determine spinnability of a melt filled with RGO, its rheological properties were determined. The neatness of the PET melt and melt when RGO is added is demonstrated through flow curves in figure 6.

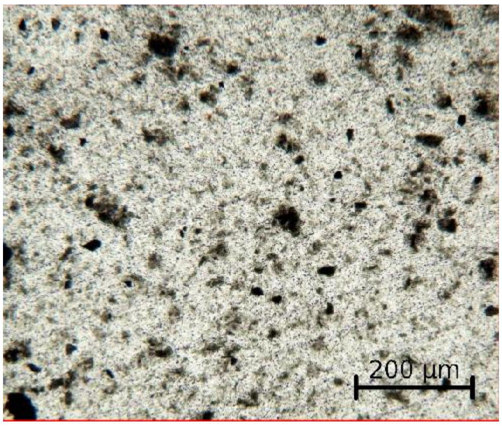

101 102 103 104 105

Figure 5. Microphotograph of RGO-PET

Figure 6. Flow curves of PET and RGO-PET

This shows how the melt of PET behaves almost Newtonianly, and that high shear stresses cause it to flow unstable. The rheological properties of PET undergo significant changes when 0. 5% is present. E. g. The viscosity of RGO PET is much higher than that of native PET at low stresses. Shear stress increased, and viscosity decreased after the short branch of constancy. It appears that the mobility of PET macromolecules is restricted by the presence of RGO particles. Grafting PET macromolecules on RGO sheets is believed to create contact forces of chemical nature with macro molecules on the RGO surface, making this explanation highly likely. Furthermore, it is possible to have partial physical interactions between solid particles, but the percolation threshold of 0. 5% of filler content could not be surpassed.

Conclusion

In situ melt poly condensation and the simultaneous reduction of GO to form RGO PET composite from the monomer and DISPERSION were achieved. The RGO PET composites created by blending graphene and PET have similar thermal properties to the one described earlier. The addition of RGO results in higher crystallinity and lower crystallization temperature, as well as a lower melt temperature. ' The temperature during the glass transition in RGO PET is lower than that of pristine PET. The strongly bonded macromolecules of PET are depicted as RGO, which is extracted from the RGO PET composite and demonstrated by TGA, XPS, and then RD. The physiological. RGO PET was investigated in its behavior. The viscosity of RGO PET is notably higher than that of neat PE, even at low stresses, and decreases as shear stress increases.

PET
RGO-PET

Acknowledgment:

Author is thankful to the technical staff of Department of Plastic Technology, School of Chemical Technology, H B Technical University, Kanpur for their support and cooperation.

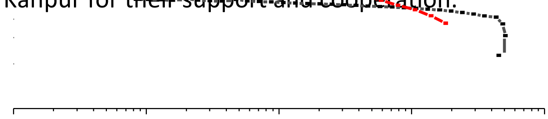

References

1. Xiao S-P and Huang H-X 2018 In situ vitamin C reduction of graphene oxide for preparing flexible TPU nanocomposites with high dielectric permittivity and low dielectric loss. Polymer Testing 66 334 https://doi.org/10.1016/j.polymertesting.2018.01.026
2. Hummers Jr W S and Offeman R E 1958 Preparation of graphitic oxide. J. of the American Chemical Society 80 1339 https://doi.org/10.1021/ja01539a017
3. Cobos M, González B, Fernández M J and Fernández M D 2018 Study on the effect of graphene and glycerol plasticizer on the properties of chitosan-graphene nanocomposites via in situ green chemical reduction of graphene oxide. Int. J. of Biological

Macromolec. 114 599 https://doi.org/10/gdrqvz

4. Soares C P P, Baptista R de L and Cesar D V 2017 Solvothermal Reduction of Graphite Oxide Using Alcohols. Mater. Res. 21 https://doi.org/10.1590/1980-5373-mr-2017-0726
5. Wan T and Chen D 2019 In Situ Reduction of Graphene Oxide in Waterborne Polyurethane Matrix and the Healing Behavior of Nanocomposites by Multiple Ways. J. of Polymer Sci.Part B 57 202 https://doi.org/10/gfw35h
6. Zhang J, He Y, Zhu P, Lin S, Ju S and Jiang D 2019 In situ reduction of graphene oxide in the poly (vinyl alcohol) matrix via microwave irradiation. Polymer Composites 40 170 https://doi.org/10/gfw35g
7. Glover A J, Cai M, Overdeep K R, Kranbuehl D E and Schniepp H C 2011 In Situ Reduction of Graphene Oxide in Polymers. Macromolec. 44 9821 https://doi.org/10.1021/ma2008783
8. Yang H, Yu Z, Wu P, Zou H and Liu P 2018 Electromagnetic interference shielding effectiveness of microcellular polyimide/in situ thermally reduced graphene oxide/carbon nanotubes nanocomposites. Appl. Surf. Sci. 434 318 https://doi.org/10.1016/j. apsusc.2017.10.
9. Yang H, Li Z, Zou H and Liu P 2017 Preparation of porous polyimide/in-situ reduced graphene oxide composite films for electromagnetic interference shielding. Polymers for Adv.Technologies 28 233 https://doi.org/ 10. 1002/pat.3879
10. Zheng D, Tang G, Zhang H-B, Yu Z-Z, Yavari F, Koratkar N, Lim S-H and Lee M-W 2012 In situ thermal reduction of graphene oxide for high electrical conductivity and low percolation threshold in polyamide 6 nanocomposites. Composite Sci. and Technol. 72 284 https://doi.org/10.1016/j.compscitech. 2011. 11.014
11. Liu K, Chen L, Chen Y, Wu J, Zhang W, Chen F and Fu Q 2011 Preparation of polyester/reduced graphene oxide composites via in situ melt polycondensation and simultaneous thermo-reduction of graphene oxide J. of Material Chemistry 21 8612 https://doi.org/10.1039/c1jm10717h
12. Marcano D C, Kosynkin D V, Berlin J M, Sinitskii A, Sun Z, Slesarev A, Alemany L B, Lu W and Tour J M 2010 Improved Synthesis of Graphene Oxide. ACS Nano 4 4806 https://doi.org/10.1021/nn1006368
13. Mikhaylov P A, Levin I S, Lubenchenko A V, Bondarenko G N and Kulichihin V G 2019 Ultrasonication-assisted ultrafast solvothermal reduction of graphene oxide. Mater. Sci. and Eng. 10 https://doi.org/10.1088/1757-899X/525/1/012039
14. Zhou T, Chen F, Liu K, Deng H, Zhang Q, Feng J and Fu Q 2011 A simple and efficient method to prepare graphene by reduction of graphite oxide with sodium hydrosulfite. Nanotechnology 22 045704 https://doi.org/10/dr9jpj
15. Kim D, Yang S J, Kim Y S, Jung H and Park C R 2012 Simple and cost-effective reduction of graphite oxide by sulfuric acid. Carbon 50 3229 https://doi.org/10. 1016
16. Awad S A and Khalaf E M 2018 Improvement of the chemical, thermal, mechanical and morphological properties of polyethylene terephthalate-graphene particle composites. Bulletin of Mater. Sci. 41 https://doi.org/10.1007/s12034-018-1587-1
17. Lubenchenko A V, Batrakov A A, Pavolotsky A B, Lubenchenko O I, Ivanov D A, 2018 XPS study of multilayer multicomponent films. Applied Surface Sci. Part A 427 711 https://doi.org/10.1016/j.apsusc.2017.07.256
18. Aoyama S, Park Y T, Ougizawa T and Macosko C W 2014 Melt crystallization of poly (ethylene terephthalate): Comparing addition of graphene vs. carbon nanotubes. Polymer 55 2077 https://doi.org/10.1016/j.polymer.2014.02 .055